# Off-resonant Raman transitions impact in an atom interferometer

Alexandre Gauguet, Tanja Mehlstäubler, Thomas Lévèque, J. Le Gouët, Oualid Chaibi, B. Canuel, Andre Clairon, Franck Pereira dos Santos, Arnaud Landragin

# Off-resonant Raman transitions impact in an atom interferometer

A. Gauguet, T. E. Mehlstäubler*, T. Lévèque, J. Le Gouët†, W. Chaibi,
B. Canuel‡, A. Clairon, F. Pereira Dos Santos, and A. Landragin§
*LNE-SYRTE, UMR 8630 CNRS, Observatoire de Paris,*
*UPMC, 61 avenue de l'Observatoire, 75014 Paris, FRANCE*
(Dated: August 29, 2008)

We study the influence of off-resonant two photon transitions on high precision measurements with atom interferometers based on stimulated Raman transitions. These resonances induce a two photon light shift on the resonant Raman condition. The impact of this effect is investigated in two highly sensitive experiments: a gravimeter and a gyroscope-accelerometer. We show that it can lead to significant systematic phase shifts, which have to be taken into account in order to achieve best performances in term of accuracy and stability.

## I. INTRODUCTION

In the field of atom interferometry, the improving sensitivity of inertial sensors [1, 2, 3, 4] is paving the way for many new applications in geophysics, navigation and tests of fundamental physics. Most of these experiments are based on Raman transitions [5] to realize beamsplitters and mirrors, which manipulate the atomic wave-packets. Among others, this technique has the advantage of an internal state labelling of the exit ports of the interferometer [6], enable an efficient detection methods. Moreover, the atoms spend most of the time in free fall, with very small and calculable interactions with the environment. The inertial forces are then determined by the relative displacement of the atomic sample with respect to the equiphases of the laser beams, which realise a very accurate and stable ruler. This makes this technique suitable for high precision measurements, as required for instance for inertial sensors and for the determination of fundamental constants [7, 8, 9, 10, 11].

A limit to the accuracy and the long term stability of these sensors comes from wave-front distortions of the laser beams. This wave-front distortion shift appears directly on the signal of an interferometer when the atoms experience different wave-fronts at each Raman pulse. This effect thus depends on the actual trajectories of the atoms, so that a precise control of the initial position, velocity and temperature of the atomic clouds is required [12, 13]. A convenient technique to reduce this bias is to minimize the number of optical components in the shaping of the two Raman laser beams and by implementing them in a retro-reflected geometry [1, 3, 14]. Indeed, as long as the two beams travel together, wave-front aberrations are identical for the two beams and thus have no influence on their phase difference. This geometry also provides an efficient way to use the $\mathbf{k}$ reversal technique, which allows to diffract the atomic wavepackets in one or the opposite direction and thus to separate effects of many major systematic errors such as gradients of magnetic fields or light shifts [15]. The main drawback of this geometry arises from the presence of off-resonant Raman transitions, which induce a light shift on the resonant Raman transition and thus a phase shift of the atom interferometer.

In the following, we investigate this effect called two photon light shift (TPLS) [16]. We first show that the TPLS arises from several off-resonant transitions and evaluate each contribution. We then derive the impact onto the phase of an atom interferometer and use our gravimeter and gyroscope-accelerometer for quantitative comparisons. In particular we measure the systematic shifts and we investigate the influence on the long term stability. The study demonstrates that the precise control of experimental parameters, in particular the Raman laser intensities and polarisations, is needed to reduce the influence of this effect for such interferometers.

* Present address: Physikalisch-Technische Bundesanstalt, Bundesallee 100, D-38116 Braunschweig, Germany
† Present address: Optical and Quantum Communications Group, MIT, Rm 36-479,Cambridge, MA 02139, USA
‡ Present address: European Gravitational Observatory, Via E. Amaldi, 56021 S. Stefano a Macerata - Cascina (PI), Italy
§arnaud.landragin@obspm.fr

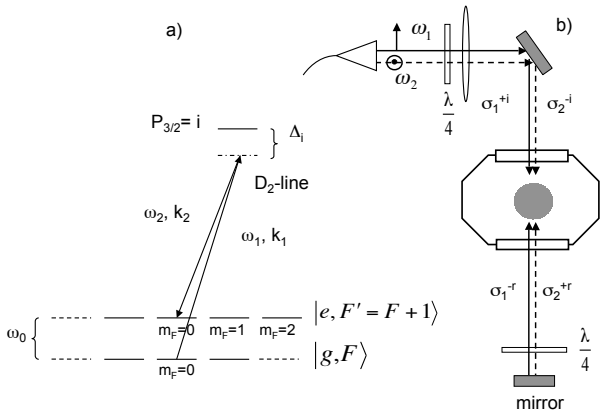


FIG. 1: Scheme of our Raman laser setup. a) Scheme of the Raman transition between the two hyperfine ground states of an alkaline atom. b) Implementation of the Raman laser beams. The two Raman lasers of orthogonal polarisations are guided to the experiment through the same polarization maintaining fibre. The two lasers are represented respectively by the solid and dashed lines. The lasers go through a first quater-wave plate ($\lambda/4$), cross the experiment and are reflected by a mirror, crossing twice a second quater-wave plate. The wave-plates are set in such a way that counter-propagating Raman transitions are allowed but co-propagating Raman transitions are forbidden.

## II. LIGHT SHIFT DUE TO OFF-RESONANT RAMAN TRANSITIONS

### A. Raman Spectroscopy

The two experiments are using different alkali-metal atoms: $^{87}$Rb in the case of the gravimeter and $^{133}$Cs in the case of the gyroscope. As hyperfine structures, transition selection rules and Raman laser setups are similar (see figure 1), their results can be compared easily. The Raman transitions couple the two hyperfine ground states of the alkaline atom (labelled $|g\rangle$ and $|e\rangle$) via an intermediate state (labelled $|i\rangle$) and two lasers with frequencies (labelled $\omega_1$ and $\omega_2$) detuned by $\Delta_i$ on the red of the $D_2$ line. During the interferometer sequence, a bias magnetic field is applied along the direction of propagation of the Raman laser beam to lift the degeneracy of the magnetic sublevel manifold. The two Raman lasers are overlapped with orthogonal linear polarisations and delivered within the same polarisation maintaining optical fiber to the vacuum chamber. After the fiber, the Raman beams pass through a quarter-wave plate to convert the initial linear polarisations into circular polarisations, noted $\sigma_1^{i+}$ for the Raman laser at the frequency $\omega_1$ and $\sigma_2^{i-}$ for the orthogonal polarisation at $\omega_2$. These beams are then retro-reflected through a quarter-wave plate to rotate the polarisation of each beam into its orthogonal polarisation ($\sigma_2^{+r}$, $\sigma_1^{-r}$).

For $m_F = 0$ to $m_F = 0$ transitions, there are two pairs of beams ($\sigma^+/\sigma^+$ and $\sigma^-/\sigma^-$), which can drive counter-propagating Raman transitions with effective wave-vectors $\pm\mathbf{k}_{\text{eff}} = \pm(\mathbf{k}_1 - \mathbf{k}_2)$. Then, the ground state $|g, \mathbf{p}\rangle$ is coupled with the excited state $|e, \mathbf{p} + \hbar\mathbf{k}_{\text{eff}}\rangle$ by the pair of Raman laser ($\sigma_1^{+i}/\sigma_2^{+r}$) and to the excited state $|e, \mathbf{p} - \hbar\mathbf{k}_{\text{eff}}\rangle$ with the pair of Raman laser ($\sigma_2^{-i}/\sigma_1^{-r}$).

We use the Doppler effect to lift the degeneracy between the two resonance conditions. Indeed, if the atoms have a velocity in the direction of propagation of the Raman lasers, the Doppler shifts are of opposite sign for the two counter-propagating transitions. The resonance condition for each of these couplings is $\Delta\omega_{\text{laser}} = \omega_0 + \omega_{\text{r}} \pm \omega_{\text{D}}$, where $\omega_0$ is the hyperfine transition frequency, $\hbar\omega_{\text{r}} = \hbar k_{\text{eff}}^2/2m$ is the recoil energy and $\omega_{\text{D}} = -\mathbf{k}_{\text{eff}}.\mathbf{v}$ the Doppler shift due to the atomic velocity $\mathbf{v}$ in the reference frame of the apparatus. Consequently, the detuning between the two resonances is $2\omega_{\text{D}}$, therefore we can discriminate between the two transitions when the Doppler shift is large enough compared to the linewidth of the Raman transition. This linewidth is characterised by the effective Rabi frequency $\Omega_{\text{eff}}$, which depends on the product of the two Raman lasers intensities and inversely to the Raman detuning $\Delta_i$ [15].

In this first part, we use the gyroscope-accelerometer experiment described in detail in [3]. The experiment has been performed with a cloud of cold Caesium atoms (1.2 $\mu K$) prepared initially in the $|F = 3, m_F = 0\rangle$ state. The atoms are launched at 2.4 m.s$^{-1}$ with an angle of 8° with respect to the vertical direction. The Raman lasers are implemented in the horizontal plane with a 6° angle with the normal of the atomic flight direction. Thus, to select only one Raman transition for the interferometer, the frequency difference between the two Raman lasers can be tuned to be resonant with either the $+k_{\text{eff}}$ or the $-k_{\text{eff}}$ transition.

Figure 2 shows the transition probability as a function of the detuning of the Raman transition with respect to the

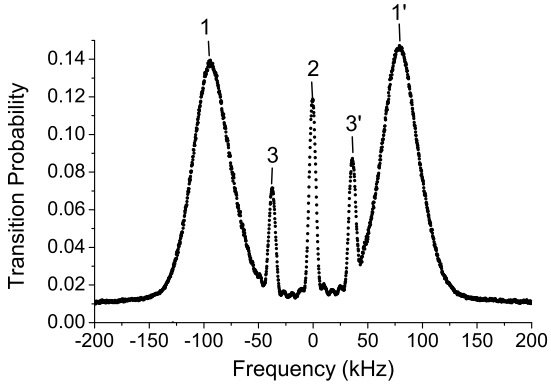


FIG. 2: Transition probability as a function of the frequency difference between the two Raman lasers when the atoms have a non-zero velocity in the direction of propagation of the Raman laser beams. The frequency is referenced to the microwave hyperfine transition ($\omega_0$). The data have been recorded with laser parameters corresponding to a $\pi$ pulse of 135 $\mu$s duration. Lines (1,1') correspond to the two counter-propagating transitions, line 2 to the copropagating transition between the two $m_F = 0$ states and lines 3 to the copropagating magnetic sensitive transitions.

hyperfine transition frequency. One can identify the two velocity selective counter-propagation transitions (labelled 1 and 1'), whose widths reflect the velocity distribution of the atomic cloud. In addition to the counter-propagating transitions, we observe transitions due to residual co-propagating Raman coupling, also detuned from resonance by a Doppler shift (lines 2, 3 and 3'). When the frequency difference of the Raman lasers is tuned to be resonant with one of the counter-propagating transitions, the second counter-propagating transition and the co-propagating ones induce a light shift (TPLS) on the selected Raman transition used for the interferometer.

### B. Frequency shift due to the 2nd pair of Raman laser beams

The TPLS is the differential shift between the two atomic levels corresponding to the atomic states $|g, \mathbf{p}\rangle$ and $|e, \mathbf{p} \pm \hbar\mathbf{k}_{\text{eff}}\rangle$ involved in the atomic interferometer. The energy of the state $|g, \mathbf{p}\rangle$ is shifted of $\varepsilon_g$ by the off-resonant $|g, \mathbf{p}\rangle \leftrightarrow |e, \mathbf{p} \mp \hbar\mathbf{k}_{\text{eff}}\rangle$ transition detuned by $\pm 2\omega_{\text{D}}$ (eq. 1), while the energy of the state $|e, \mathbf{p} \pm \hbar\mathbf{k}_{\text{eff}}\rangle$ is shifted of $\varepsilon_e$ by the off-resonant $|e, \mathbf{p} \pm \hbar\mathbf{k}_{\text{eff}}\rangle \leftrightarrow |g, \mathbf{p} \mp 2\hbar\mathbf{k}_{\text{eff}}\rangle$ transition detuned by $\hbar(\mp 2\omega_{\text{D}} + 4\omega_r)$ (eq. 2). The two levels are shifted in opposite directions as illustrated in figure 3, here for the case of a Raman transition resonant with $+\mathbf{k}_{\text{eff}}$.

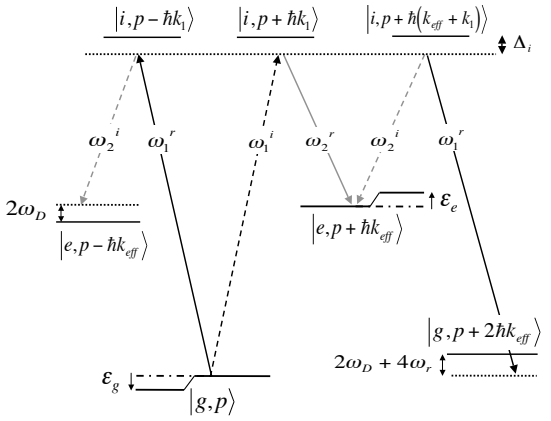


FIG. 3: Scheme of the effect on the non-resonant coupling on the two atomic states $|g, \mathbf{p}\rangle$ and $|e, \mathbf{p} + \hbar\mathbf{k}_{\text{eff}}\rangle$ involved in the atomic interferometer. The two states are coupled together through the selected Raman transition ($+\mathbf{k}$ in this particular case). But each state is also coupled to an other one, through an off-resonant Raman transition of opposite wave-vector.

TPLS corrections are calculated from fourth order perturbation theory. In the case of our system, the level shifts

$\varepsilon_g$ and $\varepsilon_e$ for a $\pm k_{\rm eff}$ interferometer are given by:

$$\varepsilon_g = \mp\hbar\frac{\Omega_{\rm eff}^2}{4\ (2\omega_{\rm D})} \tag{1}$$

$$\varepsilon_e = \hbar\frac{\Omega_{\rm eff}^2}{4(\pm 2\omega_{\rm D}+4\omega_{\rm r})}, \tag{2}$$

where $\Omega_{\rm eff}$ is the effective Rabi frequency corresponding to counter-propagating Raman transitions. Thus, the shift of the resonance condition depends on the sign of direction of the selected Raman laser pair (i.e. $\pm k_{\rm eff}$), quadratically on the Rabi frequency and inversely to the Doppler detuning:

$$\begin{aligned}\delta\omega_{(\rm TPLS\pm)} &= \tfrac{1}{\hbar}(\varepsilon_e-\varepsilon_g)\\ &= \tfrac{\Omega_{\rm eff}^2}{\pm 8\omega_{\rm D}} + \tfrac{\Omega_{\rm eff}^2}{4(\pm 2\omega_{\rm D}+4\omega_{\rm r})}\end{aligned} \tag{3}$$

### 1. *Variation with* $\Omega_{\rm eff}$

The frequency shift is measured from fits of the spectrum lines, as displayed in figure 2, with different Raman intensities ($\Omega_{\rm eff}^2$ is proportional to the product of the intensity of the two lasers). Note that we discriminate it from the shifts independent of $\mathbf{k}_{\rm eff}$, like quadratic Zeeman effect or AC Stark shift, by alternating measurements $+k_{\rm eff}$ and $-k_{\rm eff}$, leading to a differential determination of the effect. The difference in the resonance condition $\Delta\omega = 2k_{\rm eff}v + 2\delta\omega_{\rm (TPLS)}$ depends only on the TPLS and the Doppler effect. The Doppler effect does not depend on the Rabi frequency and can be determined by extrapolating $\Delta\omega$ to $\Omega_{\rm eff}=0$. The results of these measurements are displayed in figure 4 as a function of $\Omega_{\rm eff}^2$. The curve clearly shows the quadratic dependence of the frequency shift with $\Omega_{\rm eff}$. For this experimental configuration the Doppler shift was 85 kHz, and the value of $\delta\omega_{\rm (TPLS)}$ for the largest $\Omega_{\rm eff}$ ($2\pi\times 27$ kHz at the center of the beam) is 2.1 kHz in good agreement with the expected 2.4 kHz.

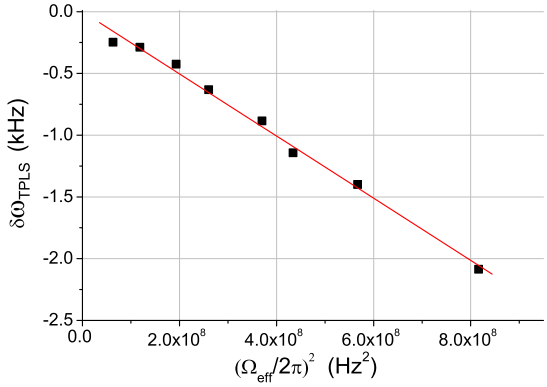


FIG. 4: Variation of the frequency shift of the counter-propagating Raman transition versus the square of the Rabi frequency. The Rabi frequency is controlled by changing the Raman laser intensities.

### 2. *Position dependance in the Raman laser beams*

The laser beams have a Gaussian shape, with a 15 mm waist (radius at $1/e^2$ in intensity). In order to evaluate the phase shift, we first measure the TPLS for different atomic positions by scanning the resonance along their trajectory. As the Raman beam are horizontal, the Doppler shift is constant for the three pulses and the TPLS varies only with the Raman laser intensity. Figure 5 displays the measured TPLS, proportional to the laser intensity, which follows exactly the Gaussian profile of the laser beams.

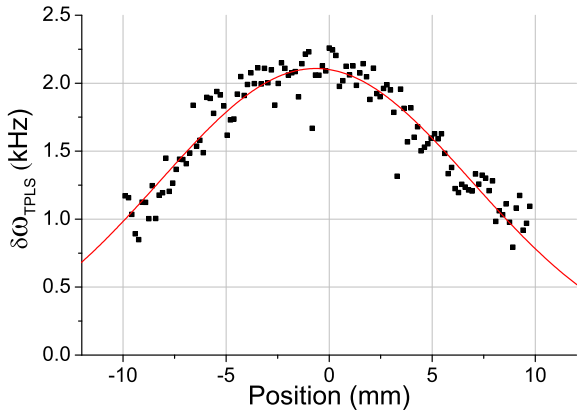


FIG. 5: Variation of the two photon light shift with the position in the Gaussian beam of the Raman lasers. The dots correspond to the measurement of the shift and the line to the fit of the data by a Gaussian function.

### C. Frequency shift due to the co-propagating transitions

In an ideal experiment, with perfect circular polarization and a Raman detuning $\Delta_i$ large compared to the hyperfine structure of the intermediate state (201 MHz in the case of the Caesium atom), co-propagating transitions are forbidden. In a real experiment, with imperfect polarization and/or finite Raman detuning, co-propagating transitions are slightly allowed, and will lead to additional TPLS.

#### *1. TPLS induced by $m_F = 0$ to $m_F = 0$ co-propagating transitions*

Imperfect polarization leads to a residual combination of $\sigma_1^+/\sigma_2^+$ and $\sigma_1^-/\sigma_2^-$ in the co-propagating beams and allows coupling between $m_F = 0$ states. As the momentum exchanged $\hbar\mathbf{k}_{\rm eff} = \hbar(\mathbf{k_1} - \mathbf{k_2}) \simeq 0$, the Doppler and recoil effect are negligible and the resonance condition is $\Delta\omega_{\rm laser} = \omega_0$ (line 2 of figure 2). The Rabi frequency corresponding to the transition $\Delta m_F = 0$ is determined experimentally using the residual co-propagating transition probability, $P = 0.1$ at full Raman laser power. It gives $\frac{\Omega_{\rm eff}}{\Omega_{00}} = 5$, which can be explained by an error of linear polarization of one of the Raman laser of 2% in power. The detuning of this transition, compared to the two counter-propagating transitions, depends on the Doppler and recoil shift:

$$\delta\omega^{00}_{(\rm TPLS\pm)} \simeq \frac{1}{4}\frac{\Omega_{00}^2}{\pm\omega_{\rm D} + \omega_{\rm r}} \tag{4}$$

For $\omega_{\rm D} = 2\pi \times 85$ kHz and $\Omega_{\rm eff} \simeq 2\pi \times 27$ kHz we find an effect due to this coupling smaller than 100 Hz.

#### *2. TPLS induced by $m_F = 0$ to $m_F = \pm 2$ co-propagating transitions*

The second source of residual co-propagating transitions stems from the coupling of $|F, m_F = 0\rangle \leftrightarrow |F', m_{F'} = \pm 2\rangle$ by the co-propagating Raman laser pairs ($\sigma_1^+$,$\sigma_2^-$) and ($\sigma_1^-$,$\sigma_2^+$). Because of the hyperfine splitting in the intermediate state, there are two paths for the Raman transition. Both transitions interfere destructively when the detuning compared to the intermediate state $\Delta_i$ is larger than the hyperfine splitting of the intermediate state, and so in this case the transition strength is zero. However, in our experimental set up, with $\Delta_i \simeq 2\pi \times 780$ MHz and the $\Delta_{HFS} = 2\pi \times 201$ MHz the ratio between the Rabi frequency of counter-propagating transitions $\Omega_{\rm eff}$ and the Rabi frequency of the co-propagating $\Delta m_F = \pm 2$ transition $\Omega_{02}$ is 6.1, leading to a transition probability of 6.4 % in good agreement with the experimental value (see figure 2). These transition resonance conditions depend on the magnetic field amplitude as $\Delta\omega_{\rm laser} = \omega_0 \pm 2\alpha B$, where $\alpha = 2\pi \times 350$ kHz/G for Caesium. With a calculation similar to the one used to obtain eq.3, we deduce the two photon light shifts $\delta\omega^{02}_{(\rm TPLS\pm)}$ induced by the magnetically sensitive transitions for the $\pm k_{\rm eff}$ case to be:

$$\delta\omega^{02}_{(\mathrm{TPLS}\pm)} = \frac{\Omega_{02}^2}{4}\left(\frac{1}{\pm\omega_\mathrm{D}+\omega_\mathrm{r}+2\alpha B} + \frac{1}{\pm\omega_\mathrm{D}+\omega_\mathrm{r}-2\alpha B}\right) \tag{5}$$

The first term in eq. 5 is due to the coupling with $|F', m_{F'} = +2\rangle$ whereas the second term is induced by the coupling with $|F', m_{F'} = -2\rangle$. It is clear from eq. 5 that a residual magnetic contribution appears in the half difference and creates a magnetic sensitivity in addition to the standard quadratic Zeeman effect. This contribution to the two photon light shift is measured by changing the bias field in the Raman interaction zone. Using the differential method previously described, we show in figure 6 the variation of the total TPLS with the bias field. The resonance around 130 mG corresponds to the case where a magnetic co-propagating transition and the counter-propagating transition are resonant simultaneously. Previous measurements have been performed with a 31 mG magnetic field bias.

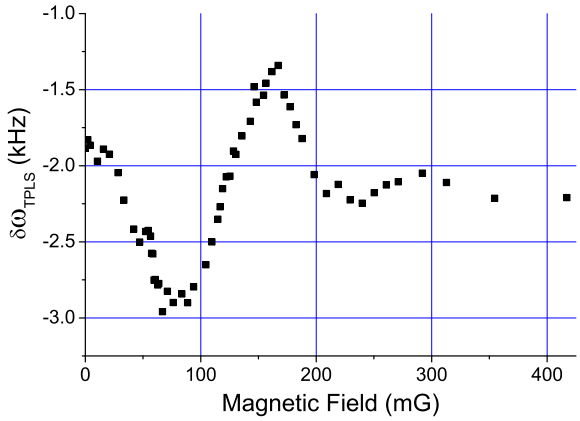


FIG. 6: Variation of the two photon light shift versus the bias magnetic field. A resonance appears when the Zeeman shift equals the Doppler shift.

## III. IMPACT ON THE INTERFEROMETER PHASE SHIFT

### A. Theoretical derivation of the phase shift

In the following we will consider interferometers constituted of three Raman pulses in a $\pi/2 - \pi - \pi/2$ sequence. If the TPLS is constant during the interferometer it is equivalent to a fixed frequency shift of the Raman transition. In that case, It is well known that no phase shift is introduced in the interferometer. On the contrary, a fluctuation of the TPLS during the interferometer sequence leads to a phase shift given by:

$$\Phi_\mathrm{TPLS} = \int_{-\infty}^{+\infty} g(t)\delta\omega_\mathrm{TPLS}(t)dt. \tag{6}$$

where $g(t)$ is the sensitivity function of the atom interferometer, defined in [17].

#### 1. *Case* $\Omega_\mathrm{eff}\tau = \pi/2$

In the case where the interaction pulses are short enough that one can neglect the variation of the TPLS during the pulses, and that the area of first and last pulse fulfils the $\Omega_\mathrm{eff}\tau = \pi/2$ condition, the two-photon interferometer phase shift can be approximated by:

$$\Phi_\mathrm{TPLS} = \left(\frac{\delta\omega^{(1)}_\mathrm{TPLS}}{\Omega^{(1)}_\mathrm{eff}} - \frac{\delta\omega^{(3)}_\mathrm{TPLS}}{\Omega^{(3)}_\mathrm{eff}}\right), \tag{7}$$

where $\omega_{\mathrm{TPLS}}^{(i)}$ and $\Omega_{\mathrm{eff}}^{(i)}$ are the TPLS and the Rabi frequencies of the i-th pulse, respectively. One might notice that the frequency shift during the $\pi$ pulse does not contribute to the interferometer phase shift. Moreover, as all components of the TPLS, counter-propagating and co-propagating terms, increase as the square of the Rabi frequencies, the interferometer phase shift scales linearly with the Raman laser power.

In the limit where the co-propagating transitions are negligible (perfect polarization and very large Raman detuning) and the dominant source of TPLS is due to the counter-propagating transition, the phase shift of the interferometer can be simplified as:

$$\Phi_{\mathrm{TPLS}}^{\mathrm{counter}} = \left( \frac{\Omega_{\mathrm{eff}}^{(1)}}{4\delta_D^{(1)}} - \frac{\Omega_{\mathrm{eff}}^{(3)}}{4\delta_D^{(3)}} \right), \tag{8}$$

where $\delta_D^i$ is the Doppler shift for the i-th pulse.

### 2. *Case* $\Omega_{\mathrm{eff}}\tau \neq \pi/2$

More generally, the interferometer phase shift can be calculated when the $\pi/2$ pulse condition is no longer fulfilled. This appears when the Rabi frequency drifts due to changes in power or polarization of the Raman lasers. Generalising the formalism of the sensitivity function to the case where $\Omega_{\mathrm{eff}}\tau \neq \pi/2$ allows deriving the interferometer phase shift:

$$\begin{aligned} \Phi_{\mathrm{TPLS}} \;=\; & \frac{\delta\omega_{\mathrm{TPLS}}^{(1)}}{\Omega_{\mathrm{eff}}^{(1)}} \tan\left( \frac{\Omega_{\mathrm{eff}}^{(1)}\tau^{(1)}}{2} \right) \\ & - \frac{\delta\omega_{\mathrm{TPLS}}^{(3)}}{\Omega_{\mathrm{eff}}^{(3)}} \tan\left( \frac{\Omega_{\mathrm{eff}}^{(3)}\tau^{(3)}}{2} \right) \end{aligned} \tag{9}$$

Usually, the Rabi frequencies and pulse durations can be taken equal for the first and the last pulses; the expression of the interferometer shift is then:

$$\Phi_{\mathrm{TPLS}} = \frac{\left( \delta\omega_{\mathrm{TPLS}}^{(1)} - \delta\omega_{\mathrm{TPLS}}^{(3)} \right)}{\Omega_{\mathrm{eff}}} \tan\left( \frac{\Omega_{\mathrm{eff}}\tau}{2} \right) \tag{10}$$

As before, for a dominant counter-propagating transition, the previous expression can be simplified to:

$$\Phi_{\mathrm{TPLS}}^{\mathrm{counter}} = \Omega_{\mathrm{eff}} \left( \frac{1}{4\delta_D^{(1)}} - \frac{1}{4\delta_D^{(3)}} \right) \tan\left( \frac{\Omega_{\mathrm{eff}}\tau}{2} \right) \tag{11}$$

An other aspect of the influence of the TPLS on the atomic phase shift concerns the stability of the experiment versus the experimental parameters fluctuations, in particular the Raman laser power. As Rabi frequency fluctuations are small in relative values (typically smaller than 10 %), we can develop eq. 11 to first order in $\delta\Omega_{\mathrm{eff}}$ close to the usual conditions $\Omega_{\mathrm{eff}}\tau = \pi/2$ and find:

$$\delta\Phi_{\mathrm{TPLS}} = \left( 1 + \frac{\pi}{2} \right) \frac{\delta\Omega_{\mathrm{eff}}}{\Omega_{\mathrm{eff}}} \Phi_{\mathrm{TPLS}} \tag{12}$$

Similar calculations may be derived to extract the dependance on the duration of the pulse or the Doppler detuning. As the stability of the latter parameters is much better controlled in cold atom interferometers, no measurable influence on the short term stability of the interferometer is expected.

## B. Case of a gravimeter

We first consider the case of the gravimeter developed at SYRTE and described in detail in [14, 18]. In this compact experimental set-up, cold $^{87}Rb$ atoms are trapped in a 3D MOT in 60 ms and further cooled during a brief optical molasses phase before being released by switching off the cooling lasers. During their free fall over a few centimetres, the interferometer is created by driving the Raman laser in the vertical direction, with pulses separated by free evolution times of $T = 50$ ms. The first Raman pulse occurs 17 ms after releasing the atoms. The Doppler

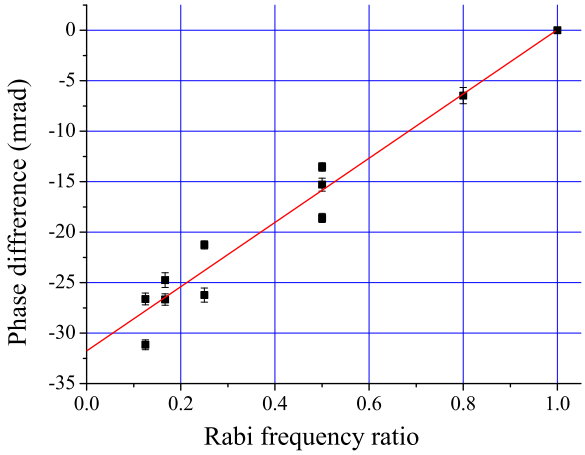


FIG. 7: Variation of the gravimeter phase shift due to the two photon light shift versus the Rabi frequency ratio, keeping the pulse area constant. To remove drifts from other sources, the phase shift is measured in a differential way by changing the Rabi frequency up to 40 kHz, which is the maximum available. The dotted line is a linear fit of the shifts.

shift at the first pulse is thus relatively small, about 400 kHz, and gets large, about 3 MHz, for the last pulse. With a Rabi frequency of 40 kHz, this leads to a TPLS of about 22 mrad for counter-propagating transition. Following the method of paragraph II C, we find a 11 mrad for co-propagating ones. This corresponds to a large shift for the gravity measurement of about $8.10^{-8}g$.

To measure the bias on the atomic interferometer phase due to TPLS, we exploit its dependence with the Rabi frequency. The principle of this measurement is based on a differential method, where one performs an alternating sequence of measurements of the interferometer phase with two different Rabi frequencies $\Omega_{\text{eff}}$ and $\Omega'_{\text{eff}}$, but keeping the areas of the pulses constant by changing the duration of the pulses $\tau$. The Rabi frequency is modulated with the power of the Raman lasers. In practice, the differential measurement is performed by alternating sequences of measurements with four different configurations : $(\Omega_{\text{eff}}, +k_{\text{eff}})$, $(\Omega_{\text{eff}}, -k_{\text{eff}})$, $(\Omega'_{\text{eff}}, +k_{\text{eff}})$ and $(\Omega'_{\text{eff}}, -k_{\text{eff}})$. After averaging for 5 minutes, we extract the difference of the TPLS between the two Rabi frequencies with an uncertainty below 1 mrad. This measurement was repeated for various $\Omega'_{\text{eff}}$, keeping $\Omega_{\text{eff}}$ fixed. The phase differences are displayed in figure 7 in according to the ratio of the Rabi frequency $\Omega'_{\text{eff}}/\Omega_{\text{eff}}$. The results clearly demonstrate the linear dependence of the phase shift with the Rabi frequency. The fit of the data allows to extract a 32 mrad shift, in very good agreement with the expected value (33 mrad), deduced from eq. 7. Deviations from the linear behavior and discrepancies (up to $\pm 10\%$) between different measurements that correspond to the same ratio cannot be explained by uncontrolled fluctuations in the Rabi frequencies, as the simultaneous monitoring of the laser intensities showed stability at the per cent level during the course of the measurements. We demonstrated that these fluctuations were correlated with changes of the polarization of the Raman beams, which modulate the contribution to the phase shift of the undesired co-propagating transitions.

We perform a complementary measurement by changing the duration of the first and last pulse simultaneously, while keeping $\Omega_{\text{eff}}$ constant. The acquisition is performed with a similar differential method than previously, but now alternating between different pulse durations and a pulse duration of 6 $\mu s$, when the $\pi/2$ pulse condition is fulfilled. The data are then shifted by the bias deduced from previous measurements with $\tau = 6$ $\mu s$ (result of figure 7) and displayed in figure 8 . Using eq. 10, the fit of the data gives a Rabi frequency of 39 kHz , in very good agreement with the expected value (42 kHz). A small deviation appears for long pulse durations when the areas of each of the two pulses is close to $\pi$.

In the case of our gravimeter, where cold atoms are dropped from rest, the TPLS is very large, almost two orders of magnitude above the pursued accuracy. In principle, this effect can be measured accurately by alternating measurements with different Rabi frequencies. But, it seems desirable to decrease the effect by operating with lower Rabi frequencies, the drawback being an increased velocity selectivity of the Raman pulses. A more stringent velocity selection, or smaller temperatures, are then required in order to preserve a good fringe contrast. In the case of a fountain gravimeter, where the atoms are launched upwards at a few m/s, the Doppler shift at the first and last pulse is much larger, considerably reducing this effect. For the parameters of the Stanford gravimeter [1] (long pulse duration of 80 $\mu$s and time between pulses of 160 ms), we find a phase shift of 0.8 mrad, which corresponds to $2.10^{-10}g$.

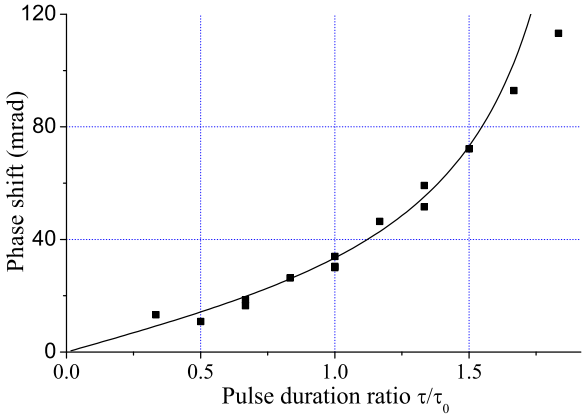


FIG. 8: Variation of the gravimeter phase due to the two photon light shift versus the pulse duration ratio, keeping the the Rabi frequency constant (40 kHz). To remove drifts from other sources, the phase shift is measured in a differential way with respect to the optimum pulse duration (6 $\mu$s). The line corresponds to the calculated shift.

### C. Case of a gyroscope-accelerometer

In the case of the gyro-accelerometer, the mean velocity of the wave-packet is not collinear with the effective Raman wave vector. Consequently, the atomic phase shift measured with the interferometer is sensitive to the rotation rate $\Omega$ in addition to the acceleration $\mathbf{a}$. As in the case of the gravimeter, the atomic phase is shifted by the TPLS and by other systematics (labelled $\Phi_0$), for instance the phase shift induced by the laser wave-front distortions [12]. The total phase shift is expressed by :

$$\Phi = \mathbf{k}_{\text{eff}} \cdot \mathbf{a}T^2 + 2\mathbf{k}_{\text{eff}} \cdot \mathbf{V} \times \mathbf{\Omega}T^2 + \Phi_0 + \Phi_{\text{TPLS}} \tag{13}$$

Our gyroscope-accelerometer uses a double interferometer with two atomic clouds following the same trajectory but with opposite directions to discriminate between acceleration and rotation phase shifts. Moreover, our experiment is designed to measure different axis of rotation and acceleration according to direction of propagation of the Raman laser beams. We will illustrate the impact of the TPLS on the interferometer in the configuration where the Raman lasers are directed along the vertical direction.

The measurement is realized in the same way than for the gravimeter experiment by comparing atomic phases with high and low Rabi frequency, changing the Raman laser power but keeping the pulse duration constant to 7.6 $\mu$s. In order to enhance the TPLS signal we decrease the time between pulses to 20 ms. Indeed, the Doppler effect is reduced and the available laser power on the side of the Gaussian laser profile is increased. The first pulse occurs 15 ms before the apogee and the third 25 ms after the apogee, corresponding respectively to a Doppler shift of about $\omega_{\text{D}}^{(1)} = 2\pi\times344$ kHz and $\omega_{\text{D}}^{(3)} = 2\pi\times574$ kHz. The Rabi frequency for each pulse is approximately 33 kHz, then the TPLS expected from eq.7 is about 38 mrad for each interferometer. As this shift is similar for the two interferometers when the two atomic clouds perfectly overlap and experiment the same TPLS, it bias the acceleration signal only. Figure 9 displays the variation of the acceleration and rotation signals with the Rabi frequency. Acceleration shift (squares) varies in a good agreement with expected shift (continuous curve) calculated from eq. 9. Rotation shift (circles) shows no dependance on the Rabi frequency and illustrates that the rejection from the acceleration signal is efficient. Nevertheless, fluctuations from expected behaviour are clearly resolved and repeatable. We attribute these deviations to wave-front distortions of the Raman laser beams. Indeed, when the atomic trajectories do no perfectly overlap, a residual bias appears on the rotation due to unperfected cancellation. This bias depends on the details of the wave-front distortions weighted by the actual atomic cloud distributions, and is modified when the Rabi frequency is changed. In the usual conditions, with interrogation time of 80 ms, the acceleration shift is reduced to about 12 mrad thanks to the increase of the Doppler shift and reduction of the Rabi frequency on the side of the Gaussian Raman beams.

We finally estimate the impact of the Raman laser power fluctuations on the stability of the rotation signal in usual conditions (interrogation time of 80 ms). We performed a complementary measurement by recording the interferometer signal and the Raman laser power in the same time when applying a modulation of the laser powers of 10%. The

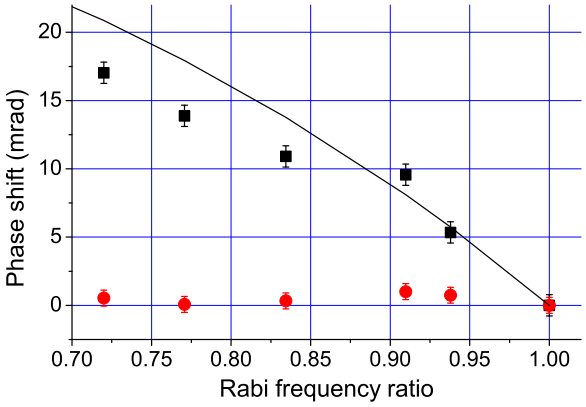


FIG. 9: Variation of the rotation and acceleration phases (resp. circles and squares) due to the two photon light shift versus the Rabi frequency ratio, keeping the pulse duration constant (7.6 $\mu$s). Acquisitions have been recorded for a total interaction time between the first and the last pulse of 40 ms. To remove drifts from other sources, the phase shift is measured in a differential way with respect to the maximum Rabi frequency available at the location of the $\pi/2$ pulses (33 kHz). The line shows the calculated shift for acceleration signal.

modulation is applied by attenuating the radio-frequency signal sends to the acousto-optic modulator used to generate the Raman pulses. The power of the lasers was recorded during the third pulse thanks to a photodiode measuring the intensity on the edge of the laser beams. We found a small dependance of the rotation signal on the power fluctuation of $6.10^{-9}$ rad.s$^{-1}$/%, which can limit the long term stability of the gyroscope. As no dependance was expected, we attribute it again to non perfect superimposition of the two atomic clouds trajectories, leading to a different Rabi frequencies experienced by the two clouds.

## IV. CONCLUSION

We have shown that the use of retro-reflected Raman lasers in atom interferometers induces off-resonant Raman transitions, which have to be taken into account in order to achieve best accuracy and stability of interferometers. We have first quantitatively evaluated the effect on the resonance condition for each off-resonant line: the other counter-propagating transition, which can not be avoided in the retro-reflected design, and co-propagating transitions arising mainly from imperfections in the polarisation. Then, we have measured the impact of this two photon light shift on the phase of two atom interferometers: a gravimeter and a gyroscope. In particular, we show that this shift is an important source of systematic errors for acceleration measurements. Nevertheless, it can be measured accurately by modulating the Raman laser power and/or the pulse durations. Our study has also shown that it can impact the stability of the two sensors if the polarization and/or the power of the Raman lasers fluctuate.

The TPLS appears as a drawback of using retro-reflected Raman laser beams. But, as it can be well controlled, it does not reduce the benefit from this geometry, whose key advantage is to drastically limit the bias due to wave-front aberrations, which is larger and more difficult to extrapolate to zero.

This study can be extended to other two photon transitions (like Bragg transitions) and to other possible polarization configurations (when using linear instead of circular polarizations), when using the Doppler effect to select the transition. If the signal is generated from the subtraction of the phase shifts of two independent atomic clouds, e.g. gradiometers or gyroscopes, perfect common mode rejection, is required to suppress this effect. In our case this means a perfect overlap of atomic trajectories.

Finally, the two photon light shift can be drastically reduced by increasing the Doppler effect and/or using colder atoms, allowing to reduce the Rabi frequency during the Raman pulses. By contrast, for set-up with intrinsic small Doppler effect, as for space applications [13, 19], this effect becomes extremely large and has to be taken into account in the design of the experiment.

**Acknowledgments**

We express our gratitude to F. Biraben for pointing out this effect and to P. Cheinet for earlier contributions to the gravimeter experiment. We would like to thank the Institut Francilien pour la Recherche sur les Atomes Froids (IFRAF), the European Union (FINAQS contract), the Délégation Générale pour l'Armement (DGA) and the Centre National d'Études Spatiales (CNES) for financial supports. B. C., J. L.G. and T. L. thank DGA for supporting their work.

[1] A. Peters, K. Y. Chung, S. Chu, Metrologia **38** 25 (2001).
[2] T. L. Gustavson, A. Landragin, M. A. Kasevich, Class. Quantum Grav. **17** 1-14 (2000).
[3] B. Canuel, F. Leduc, D. Holleville, A. Gauguet, J. Fils, A. Virdis, A. Clairon, N. Dimarcq, Ch.J. Bordé, A. Landragin, and P. Bouyer, Phys. Rev. Lett. **97**, 010402 (2006).
[4] J. M. McGuirk, G. T. Foster, J. B. Fixler, M. J. Snadden, M. A. Kasevich, Phys.Rev. A **65** 033608 (2002).
[5] M. Kasevich, D.S. Weiss, E.Riis, K. Moler, S. Kasapi and S. Chu, Phys. Rev. Lett. **66** 2297 (1991).
[6] Ch.J. Bordé, Phys. Lett. A **140**, 10 (1989).
[7] Fixler07 J. B.Fixler, G. T. Foster, J. M. McGuirk and M. A. Kasevich, Science Magazine **Vol. 315. no. 5808**, 74 (2007).
[8] G. Lamporesi, A. Bertoldi, L. Cacciapuoti, M. Prevedelli, and G. M. Tino, Phys. Rev. Lett. **100**, 050801 (2008).
[9] A. Wicht, J.M. Hensley, E. Sarajlic and S. Chu, Physica Scripta **T102**, 82 (2002).
[10] P. Cladé, E. de Mirandes, M. Cadoret, S. Guellati-Khélifa, C. Schwob, F. Nez, L. Julien and F. Biraben, Phys. Rev. Lett. **96**, 033001 (2006).
[11] G. Genevès *et al.* IEEE Trans. on Instr. and Meas. **54**, 850 (2005).
[12] J. Fils, F. Leduc, P. Bouyer, D. Holleville, N. Dimarcq, A. Clairon and A. Landragin, Eur.Phys. J. D **36**,257-260 (2005).
[13] A. Landragin and F. Pereira Dos Santos, in *Proc. of the Enrico Fermi International School of Physics* **168** (2007), in press, arXiv: 0808.3837
[14] P. Cheinet, F. Pereira Dos Santos, T. Petelski, J. Le Gouët, J. Kim, K. T. Therkildsen, A. Clairon and A. Landragin Appl. Phys. B **84**, 643 (2006).
[15] D. S. Weiss, B. C. Young and S. Chu, Appl. Phys. B **59**, 217 (1994).
[16] P. Cladé, E. de Mirandes, M. Cadoret, S. Guellati-Khélifa, C. Schwob, F. Nez, L. Julien and F. Biraben, Phys. Rev. A **74**, 052109 (2006).
[17] P. Cheinet, B. Canuel, F. Pereira Dos Santos, A. Gauguet, F. Leduc, A. Landragin, IEEE Trans. on Instr. and Meas. **57**, 1141 (2008).
[18] J. Le Gouët, T. E. Mehlstäubler, J. Kim, S. Merlet, A. Clairon, A. Landragin and F. Pereira Dos Santos, Appl. Phys. B **92**, 133-144 (2008).
[19] see for instance Apll. Phys. B **84**, number 4, Special Issue: "Quantum Mechanics for Space Application: From Quantum Optics to Atom Optics and General Relativity", P. Wolf *et al.*, accepted for publication in Experimental Astronomy, arXiv: 0711.0304v5, W. Ertmer *et al.* submitted for publication in Experimental Astronomy, and references therein.